

## Polymorphic Behavior of Structured Fats Including Stearic Acid and $\omega$ -3 Polyunsaturated Fatty Acids

Kiyotaka Sato · Tomoe Kigawa · Satoru Ueno ·  
Naohiro Gotoh · Shun Wada

Received: 7 July 2008 / Revised: 15 December 2008 / Accepted: 23 December 2008 / Published online: 24 January 2009  
© AOCS 2009

Dear Sir,

It has widely been recognized that long-chain  $\omega$ -3 polyunsaturated fatty acids ( $\omega$ -3 PUFAs) such as  $\alpha$ -linolenic acid (ALA), eicosapentaenoic acid (EPA) and docosahexaenoic acid (DHA) play critical roles in human health [1–3]. Compared with chemical and nutritional studies of the  $\omega$ -3 PUFAs, their physical properties have so far not been clarified (except for ALA) [4]. This is mainly because the  $\omega$ -3 PUFAs are liquid at ambient temperatures in a form of free fatty acid (FFA), as their low melting points are low ( $-11$  °C for ALA,  $-54$  °C for EPA and  $-44$  °C for DHA). Therefore, research to determine the physical properties of lipid materials, that are more significant in solid state or liquid-crystalline states rather than in a liquid state, has been limited [5–7]. Wijesundera et al. recently studied chemical and physical properties of triacylglycerols (TAGs), in which palmitic acid, oleic acid and DHA are esterified at various glycerol carbon positions [8, 9]. Quite interestingly, they found that oxidation of DHA was retarded when it is esterified at the *sn*-2 position rather than esterified at the *sn*-1 (or *sn*-3) position. Previous studies have shown that the melting points of the mixed-acid TAGs containing saturated fatty acids, ALA, EPA and DHA are in the range of 33–36 °C, although crystal structure data have not been reported [5–8].

In the present study, we examined basic physical properties of mixed-acid triacylglycerols (TAGs), in which stearic acid was esterified at the *sn*-1,3 positions, and ALA, EPA and DHA were esterified at the *sn*-2 carbon position in a glycerol group. Thereafter, the three TAGs are en bloc abbreviated as S-PUFA-S TAGs, and individual TAGs as S-ALA-S (1,3-stearoyl-2- $\alpha$ -linoleoyl-glycerol), S-EPA-S (1,3-stearoyl-2-eicosapentaenoyl-glycerol) and S-DHA-S (1,3-stearoyl-2-docosahexaenoyl-glycerol). The main motivation of the present work was to examine whether the melting points of the three S-PUFA-S TAGs increase compared to those in the FFA states through molecular interactions of stearic acid moieties of the S-PUFA-S TAGs. If the melting points of the S-PUFA-S TAGs are higher than ambient room temperature, we can reasonably expect that the S-PUFA-S TAGs can be utilized as solid fat materials for various edible applications. For reference, it may be worth noting that the melting points of the most stable forms of 1,3-stearoyl-2-oleoyl-glycerol (SOS) [10] and 1,3-stearoyl-2-linoleoyl-glycerol (SLS) are 43.0 and 34.5 °C [11], respectively.

The S-PUFA-S TAGs samples were purchased from Tsukishima Foods Co. Ltd. The purity of each S-PUFA-S TAG was analyzed by using high-performance liquid chromatography (HPLC), gas chromatography, and  $^1\text{H}$  and  $^{13}\text{C}$  NMR.

In HPLC, the S-PUFA-S TAG sample was subjected to an HPLC comprising a pump (LC-10A, Shimadzu, Tokyo, Japan), a tandem jointed triacontyl silyl column (DEV-ELOSIL RPAQUEOUS C-30, i.d. 5  $\mu\text{m}$ , 4.6  $\times$  250 mm, Nomura Chemical Co., Tokyo, Japan), an evaporative light-scattering detector (ELSD) (PL-ELS 1000, Varian, Inc., Palo Alto, CA), and a chromatopac integrator (C-R6A, Shimadzu, Tokyo, Japan). Acetonitrile and 2-propanol were used for the elution solvent in the gradient system. The flow

K. Sato (✉) · T. Kigawa · S. Ueno  
Graduate School of Biosphere Science, Hiroshima University,  
Kagamiyama 1-4-4, Higashi-Hiroshima 739-8528, Japan  
e-mail: kyosato@hiroshima-u.ac.jp

N. Gotoh · S. Wada  
Department of Food Science and Technology,  
Tokyo University of Marine Science and Technology,  
4-5-7 Konan, Minato-ku, Tokyo 108-8477, Japan

rate and column temperature were 0.8 mL and 20 °C. The evaporator temperature was 110 °C, the nebulizer temperature was 90 °C, and the gas flow rate of the ELSD was 1.0 mL/min.

In gas chromatography, the methyl esterified fatty acids derived from the S-PUFA-S TAG sample were tested with a gas chromatography flame ionization detector (GC-FID) system (GC14B, Shimadzu, Tokyo, Japan) equipped with a capillary column (Omegawax320, 30 m × 0.25 mm ID, Sigma-Aldrich Japan, Tokyo, Japan) and chromatopac integrator (C-R6A). The temperature of the injection port was 250 °C, and that of the detector was 260 °C. The initial column temperature was 175 °C and increased to 225 °C at a rate of 1 °C/min. Helium at a flow rate of 32 cm/s was used as the carrier gas. The fatty acid species was identified using the retention time of a fatty acid methyl ester standard solution (Supelco 37 Component FAME Mix, Sigma-Aldrich Japan, Tokyo, Japan). The relative content of respective fatty acids was calculated with a GC-FID chromatogram.

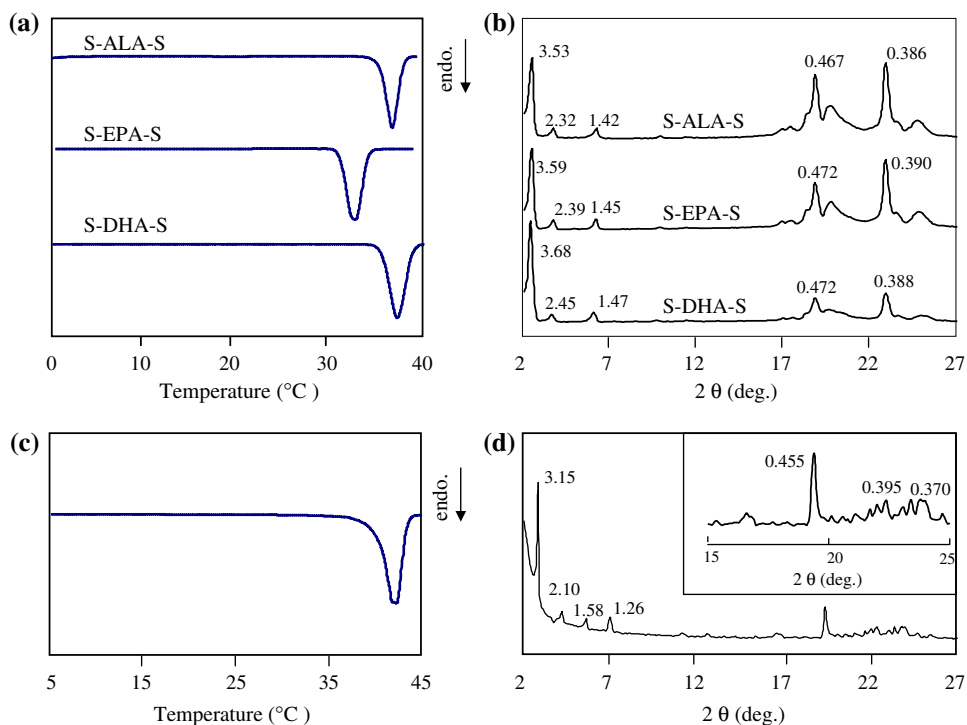
In  $^1\text{H}$  and  $^{13}\text{C}$  NMR, the S-PUFA-S TAG sample was dissolved in  $\text{CDCl}_3$ . The solution was placed in a micro NMR sample tube (CMS-005 J, Shigemi Co., Ltd., Tokyo Japan) and subjected to  $^1\text{H}$ -NMR ( $^{13}\text{C}$ -NMR) analysis (AVANCE 400 WB, Bruker, Karlsruhe, Germany) at 400 MHz (100 MHz). The  $^1\text{H}$ -NMR spectrum was acquired under the following conditions: temperature 20 °C, pulse delay 1.0 s, spectral width 8,200 Hz, acquisition time 2.0 s, 32 k data points, pulse angle 30°, and 32

scans. The  $^{13}\text{C}$ -NMR spectrum was acquired under the following conditions: temperature 20 °C, pulse delay 1.0 s, spectral width 24,000 Hz, acquisition time 1.4 s, 66 K data points, pulse angle 45°, and 128 scans.

Although not shown here, these chemical analyses demonstrated that *trans*-isomers could not be detected in the three S-PUFA-S TAGs and that the purity was guaranteed to be above 99%. Thermal differential scanning calorimetric analysis (DSC) (DSC 8240, Rigaku Co., Tokyo, Japan) and X-ray diffraction (XRD) (RINT-TTR, Rigaku Co., Tokyo, Japan) measurements were performed for the samples prepared by heating at 50 °C and cooling to −30 °C. All the samples were subjected to DSC and XRD experiments in  $\text{N}_2$  gas to prevent oxidation, and no sample was reused after an experiment run. All experiments were repeated twice to confirm reproducibility.

Figure 1 depicts DSC heating thermopeaks and XRD patterns of three S-PUFA-S TAGs acquired during heating soon after the samples were cooled from 50 to −30 °C. As indicated in the two results, the melting points of the three S-PUFA-S TAGs were not low, as one may simply assume in accordance with the melting points of the ALA, EPA and DHA in the FFA state. Surprisingly, the melting point of S-DHA-S is even higher than that of S-ALA-S, even though the melting point of DHA in FFA is far lower than that of ALA. The XRD patterns of the three S-PUFA-S TAGs exhibited very sharp peaks both in small-angle and wide-angle regions near room temperature (Fig. 1b), proving that the three S-PUFA-S TAGs are in the solid

**Fig. 1** **a** DSC heating thermopeaks (2 °C/min) of  $\gamma$  forms of three S-PUFA-S TAGs taken after cooling from 50 to −30 °C. **b** XRD patterns of  $\gamma$  forms of three S-PUFA-S TAGs taken at 10 °C (S-ALA-S), 20 °C (S-EPA-S), and 20 °C (S-DHA-S) during heating soon after cooling from 50 to −30 °C. **c** DSC heating thermopeak (2 °C/min) of  $\beta$  form of S-ALA-S after storing the sample of (a) for 6 days at 37 °C in  $\text{N}_2$  gas. **d** XRD pattern of  $\beta$  form of S-ALA-S taken at 10 °C. An inserted figure shows detailed wide-angle XRD pattern



state at ambient temperature. In particular, the XRD patterns in the small-angle region exhibited high indices of long spacing, reflecting lamellar stacking stability. For example, the XRD peaks of 3.59, 2.39 and 1.45 nm of S-EPA-S correspond to the 002, 003 and 005 reflections of the long-spacing value of  $7.16 \pm 0.02$  nm, which is stacked in a triple-chain-length structure. The intensities of XRD peaks of the three reflections increase in the order of 003, 005 and 002, which agrees quite well with the intensity ratio of the long-spacing XRD peaks of the triple-chain-length structure observed in SOS [10, 12], and proving the triple-chain-length structure of the S-ALA-S crystal. The same result was observed in S-ALA-S and S-DHA-S in Fig. 1b, although the 002 reflection of S-DHA-S is rather weak. The three S-PUFA-S TAGs exhibited almost identical XRD patterns in the wide-angle region, in which two strong peaks of 0.46–0.47 nm and 0.37–0.38 nm appeared. Compared with other saturated-unsaturated mixed-acid TAGs (e.g., SOS [10, 12, 13], SLS [11], SRS (R: ricinoleic acid) [14], and POP (1,3-palmitoyl-2-oleoyl-glycerol) [10, 13], we can conclude that the three S-PUFA-S TAGs are all  $\gamma$  polymorphic forms. The  $\gamma$  form is metastable in SOS, SRS and POP, whereas it is the most stable form in SLS. Therefore, we conclude that the polymorphic forms of S-ALA-S, S-EPA-S and S-DHA-S evolved at ambient temperature during heating soon after cooling from 50 to  $-30$  °C are  $\gamma$  forms with a triple-chain-length structure.

In the present study, we also discovered that the polymorphic transformation from  $\gamma$  form to  $\beta$  form occurred in S-ALA-S when S-ALA-S was stored for 6 days at 37 °C. Figure 1c, d illustrate the DSC melting and XRD patterns of  $\beta$  form of S-ALA-S. The melting point increased from 32.5 °C for  $\gamma$  form to 41.0 °C for  $\beta$  form. The long-spacing value of  $\beta$  form is 6.31 nm, which is shorter than that of  $\gamma$  form (7.04 nm). The XRD wide-angle peaks characterized by a strong peak of 0.455 nm and medium peaks of 0.395 nm and 0.370 nm are typical of  $\beta$  form. Although SOS and POP have two  $\beta$  forms ( $\beta_1$  and  $\beta_2$ ) [7], we cannot decide yet whether the  $\beta$  form of S-ALA-S is  $\beta_1$  or  $\beta_2$ . The triple-chain-length structure of the  $\beta$  form of S-ALA-S was demonstrated in the increasing intensity of the long-spacing patterns in the order of 2.10 nm (003), 1.58 nm (004), 1.26 nm (005) and 3.15 nm (002) (Fig. 1d). S-EPA-S and S-DHA-S did not transform from  $\gamma$  to  $\beta$  form when the crystals were kept just below their melting points of  $\gamma$  form over 1 month. Incubation of  $\gamma$  form just above its melting point may cause  $\gamma$  to  $\beta$  transformation. However, oxidation rapidly occurred during this experiment for S-EPA-S and S-DHA-S, before the transformation from  $\gamma$  to  $\beta$  was detected. Therefore, it may be too early to decide the existence or absence of  $\beta$  form in S-EPA-S and S-DHA-S, since further studies, such as incubation under oxidation-

prohibited conditions or solvent crystallization, are needed to draw any conclusions.

Table 1 compares thermal and structural data of the three S-PUFA-S TAGs with those of SOS and SLS, from which the properties can be summarized as follows:

1.  $\gamma$  and  $\beta$  forms of S-ALA-S and  $\gamma$  form of S-EPA and S-DHA-S were observed.
2. The three crystals are stacked in a triple-chain-length structure, in which stearic acid moiety and PUFA moiety are stacked in different layers (Fig. 2).
3. For  $\gamma$  forms, the long-spacing value was greatest in S-DHA-S (7.35 nm), intermediate in S-EPA-S (7.16 nm) and smallest in S-ALA-S (7.04 nm). This result is basically in good agreement with the carbon numbers (Cn) of the PUFAs; S-DHA-S (Cn = 22), S-EPA-S (Cn = 20) and S-ALA-S (Cn = 18). The long-spacing value of the  $\gamma$  form of SOS was almost the same as that of S-ALA-S but shorter than that of SLS by 0.2 nm.
4. The difference in the long-spacing values between S-ALA-S and S-EPA-S is 0.12 nm, and that between S-EPA and S-DHA-S is 0.19 nm. These differences are rather small compared with the differences in the chain length of the saturated fatty acids, in which chain lengths differ by 0.25 nm by increasing Cn by 2, if the fatty acid chains are arranged normal to the lamellar plane and their conformation are in all *trans*. This result indicates that the molecular conformation of the PUFA moiety in the triple-chain-length structure illustrated in Fig. 2 may not be in a stable *trans* state.
5. The melting points of the three S-PUGA-S TAGs are in good agreement with those previously reported [5–7] and these values are surprisingly higher than the melting points of PUFAs in the FFA state. The melting

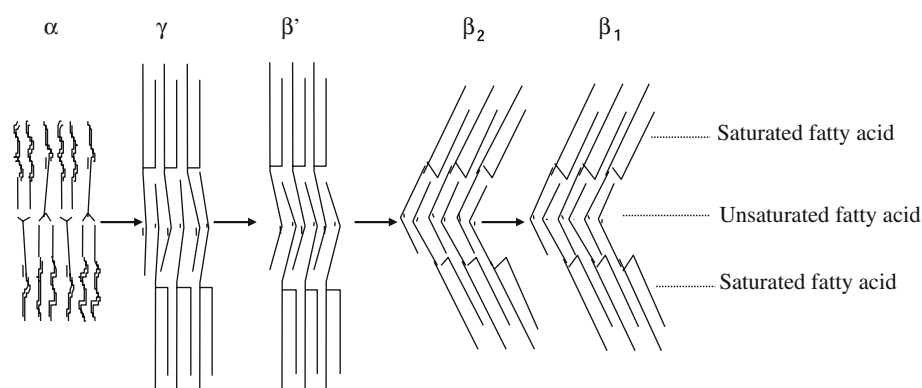
**Table 1** Thermal and long spacing (LS) data of three S-PUFA-S TAGs, SOS and SLS

TAGs	Polymorph	m.p. (°C) <sup>a</sup>	DH (kJ/mol)	DS (J/mol/K)	LS (nm) (error $\pm$ 0.02 nm)
S-DHA-S	$\gamma$ form	36.2	130.2	421.3	7.35
S-ALA-S	$\gamma$ form	35.9	116.2	374.6	7.04
	$\beta$ form	40.1	138.7	438.8	6.31
S-EPA-S	$\gamma$ form	32.5	116.7	379.6	7.16
S-O-S	$\gamma$ form	35.4	98.5	319.2	7.05
	$\beta_1$ form	43.0	151.0	477.6	6.50
S-L-S	$\gamma$ form	35.0	137.2	445.2	7.33

m.p. melting point, DH enthalpy of fusion, DS entropy of fusion, LS long spacing

<sup>a</sup> S-ALA-S (1,3-stearoyl-2-a-linoleoyl-glycerol), S-EPA-S (1,3-stearoyl-2-eicosapentaeneoyl-glycerol), S-DHA-S (1,3-stearoyl-2-docosa-hexaenoyl-glycerol), SOS (1,3-stearoyl-2-oleoyl-glycerol) and SLS (1,3-stearoyl-2-linoleoyl-glycerol)

**Fig. 2** Molecular models of five polymorphic forms of SOS



points of the  $\gamma$  forms of the five TAGs are almost the same, and the  $\beta$  forms of SOS and S-ALA-S exhibited the same traits.

The above results support the following important conclusions. (a) In the mixed-acid TAGs, the PUFA and stearic acid moieties form different layers, resulting in the triple-chain-length structure. (b) Because of the strong van der Waals interactions between the stearic acid layers of the triple-chain-length structure, the ALA, EPA and DHA layers may exhibit extended chain conformation to produce long-spacing values around 6 to 7 nm as illustrated in Fig. 2. If the PUFAs are in a disordered kink conformation, such large long-spacing values should not be obtained. (c) As a result, the melting points of the three S-PUFA-S TAGs are actually decided by van der Waals interactions among the stearic acid moiety and become much higher than those of PUFAs in the FFA state.

The present preliminary results have demonstrated that PUFAs can be utilized as solid fats if they are structured at the *sn*-2 position together with stearic acid, which is structured at the *sn*-1 and *sn*-3 positions. This may also let us conceive a variety of molecular interactions and fat blending with other solid fats, bioavailability of the *sn*-2 PUFAs after melting of PUFA-including solid fats in our body, and oxidative stability of solid PUFAs. To achieve these expectations, further research on the crystals of the S-PUFA-S TAGs, such as their detailed molecular structures, mixing properties with other fats, and oxidative stability, is needed.

## References

- Cunnane SC (2003) Problems with essential fatty acids: time for a new paradigm? *Prog Lipid Res* 42:544–568
- Schmitz G, Ecker J (2008) The opposing effects of n-3 and n-6 fatty acids. *Prog Lipid Res* 47:147–155
- Hamazaki T, Hamazaki K (2008) Fish oil and aggression or hostility. *Prog Lipid Res* 47:221–232
- Ueno S, Miyazaki A, Yano J, Furukawa Y, Suzuki M, Sato K (2000) Polymorphism of linoleic acid (*cis*-9, *cis*-12-Octadecadienoic acid) and  $\alpha$ -linolenic acid (*cis*-9, *cis*-12, *cis*-15-Octadecatrienoic acid). *Chem Phys Lipids* 107:169–178
- Serebrennikova GA, Mitrofanov TK, Kraevski AA, Sarychev IK, Preobrazhenski NA (1961) Total synthesis of triglycerides of soybean oil. *Doklady Chem* 140:1008–1011 (S-ALA-S, 36C)
- Haraldsson GG, Halldorsson A, Kulas E (2000) Chemoenzymatic synthesis of structured triacylglycerols containing eicosapentaenoic and docosahexaenoic acids. *J Am Oil Chem Soc* 77:1139–1145 (S-DHA-S 35-35.5C) (S-EPA-S 33.5-34C)
- Adlof RO, List GR (2003) Synthesis and analysis of symmetrical and nonsymmetrical disaturated/monounsaturated triacylglycerols. *J Agric Food Chem* 51:2096–2099 (S-ALA-S 36.5C)
- Fraser BH, Perlmutter P, Wijesundera C (2006) Practical syntheses of triacylglycerol regioisomers containing long-chain polyunsaturated fatty acids. *J Am Oil Chem Soc* 84:11–21
- Wijesundera C, Ceccato C, Watkins P, Fagan P, Fraser B, Thienthong N, Perlmutter P (2008) Docosahexaenoic acid is more stable to oxidation when located at the *sn*-2 position of triacylglycerol compared to *sn*-1(3). *J Am Oil Chem Soc* 85:543–548
- Sato K, Arishima T, Wang ZH, Ojima K, Sagi N, Mori H (1989) Polymorphism of POP and SOS. I. Occurrence and polymorphic transformation. *J Am Oil Chem Soc* 66:664–674
- Takeuchi M, Ueno S, Yano J, Floeter E, Sato K (2000) Polymorphic transformation of 1,3-distearoyl-*sn*-linoleoyl-glycerol. *J Am Oil Chem Soc* 77:1243–1249
- Mykhaylyk OO, Smith KW, Martin CM, Ryan AJ (2007) Structural models of metastable phase occurring during the crystallization process of saturated/unsaturated triacylglycerols. *J Appl Cryst* 40:S297–S302
- Rousset P, Rappaz M (1996) Crystallization kinetics of the pure triacylglycerols: glycerol-1,3-dipalmitate-2-oleate, glycerol-1-palmitate-2-oleate-3-stearate, and glycerol-1,3-distearate-2-oleate. *J Am Oil Chem Soc* 73:1051–1057
- Boubekri K, Yano J, Ueno S, Sato K (1999) Polymorphic Transformations in SRS (*sn*-1,3-distearoyl-2-ricinoleyl glycerol). *J Am Oil Chem Soc* 76:949–955